3-D Positioning Tasks for RUAS Using Switched PVTOL Controllers

Alexandre S. Brandão
Department of Electrical Engineering
Federal University of Viçosa
Viçosa - MG, Brazil
Email: alexandre.brandao@ufv.br

Mário Sarcinelli Filho
Department of Electrical Engineering
Federal University of Espírito Santo
Vitória - ES, Brazil
Email: mario.sarcinelli@ufes.br

Claudio D. Rosales and Ricardo Carelli
Instituto de Automática
National University of San Juan
San Juan, Argentine
Email: {crosales,rcarelli}@inaut.unsj.edu.ar

***Abstract*—In this work a switching strategy associated to three PVTOL controllers is proposed to guide a rotorcraft during 3-D navigation. The proposal is to orientate the rotorcraft to the desired point (using a Z-PVTOL controller) and then to move it ahead (using a XZ-PVTOL controller), considering the body reference frame. In such goal search, if a lateral displacement error greater than a threshold value is observed an YZ-PVTOL controller is run to minimize it. The stability proof for each of such sub-systems is also included, as well as a strategy to switch between them without affecting the stability of the whole system. Finally, experimental results are presented to validate the proposed approach and its performance during a flight mission is compared to the performance of a controller based on partial nonlinear feedback, proposed to control all degrees of freedom simultaneously.**

I. Introduction

It is noticeable the great interest of the scientific community in unmanned aircraft systems (UAS) in recent years. This is mainly for some characteristics of such aircrafts that facilitate the accomplishment of certain tasks, in a large variety of areas, such as public safety (e.g., aerial space and urban traffic supervision), natural risk management (e.g. monitoring of active volcanos), environmental management (e.g., air pollution measurement and forest supervision), interventions in hostile environments (e.g., radioactive atmospheres), infrastructure maintenance (e.g., supervision of transmission lines and fluid or gas pipes) and precision agriculture (e.g., detection and treatment of infested cultivations). In such applications the use of UAS is extremely advantageous in comparison to the use of unmanned ground vehicles (UGVs), because of their tridimensional mobility [1]–[4].

Most of these applications require low-altitude flight with hovering and vertical take-off and landing (VTOL) capabilities, and small rotorcraft unmanned aircraft systems (RUAS) are more appropriate for these applications than fixed-wing UAS [5]. This is because a crucial feature of the helicopter is to be functionally controllable in the lateral/longitudinal and vertical directions with arbitrary yaw-attitude. This feature guarantees high maneuverability to the helicopter, which is a feature distinguishing this kind of aircraft from the fixed-wing ones [6]. A disadvantage is, however, a relatively higher power consumption during the flight. Regarding the rotorcraft families, a quadrotor is much simpler and easier to build, compared to a classical helicopter, since it has no swashplate and is controlled by varying only the angular velocity of each of the four motors, making this system very attractive to experience control strategies.

The control of the RUAS has attracted the attention of many researchers from both the control and robotics communities, because it presents interesting control challenges and a good chance to develop and test new control strategies. A great variety of papers about RUAS control is yet available in the literature. Some of them are based on adaptive control, like that in [7], where the authors propose a nonlinear adaptive controller for vision-based flight with a quadrotor. Other works use backstepping technique, like the one in [8]. In [9], the developed algorithm generates optimal trajectories trough a sequence of 3D positions and yaw angles. These trajectories are then accurately tracked using a nonlinear inner- and outer loop controller. In [10] it is proposed a real-time non-linear nested saturation control scheme based on Lyapunov's stability criterion. In [11] and [12] a under-actuated controller has been proposed. In [13] the authors compared the performance of their non-linear controller with a linear one, such as LQR, which presents stability issues when the system is taken far away from the operation point used to design the controller.

All these works, as well as many others, are based on the nonlinear model of the helicopter, which many times makes the implementation of these control laws not easy, either because the computational demand of the algorithm is too much, or because the degree of ideality is such that it is impossible to experiment outside the laboratory. An alternative to this has been presented in [14], where the authors introduced the concept of planar vertical takeoff and landing (PVTOL) tasks, which is an important benchmark for control design, aiming at stabilizing a rotorcraft in a vertical axis (or plane). This model is based on limiting some degrees of freedom of the system, and according to the limited variables different PVTOL models are generated. If the task is performed in the XZ plane, for instance, the yaw and roll movements should be restricted. When the task is to be accomplished in the YZ plane, the yaw and pitch movements should be restricted. On the other hand, if a VTOL task (hovering task) is required, the lateral and longitudinal movements should be restricted but not the yaw movement.

978-1-4673-1388-9/13/$31.00 ©2013 IEEE

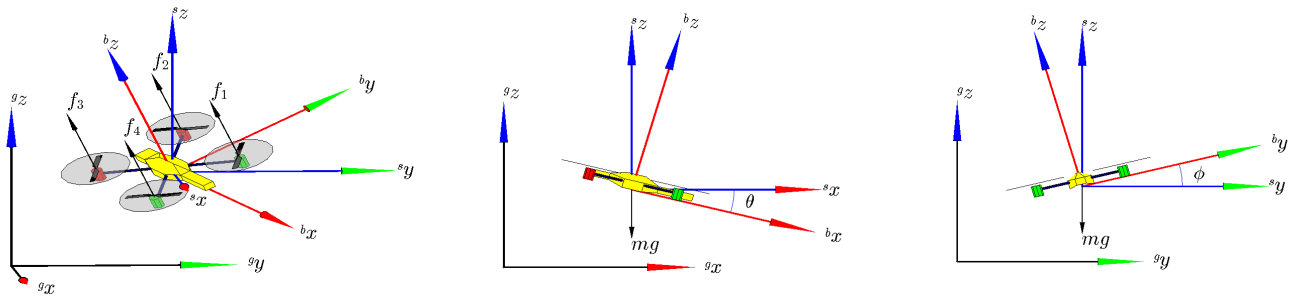

(a) (b) (c)

Fig. 1. Rotary unmanned aerial system. (a) 6-DOF model of an ArDrone quadrotor, with the reference system and the abstracts control inputs f_i associated to it. The inertial, spatial and body frame are $\langle g \rangle$, $\langle s \rangle$ and $\langle b \rangle$, as indicated by the left superscript in the axes x, y and z. (b) (c).

A property of the PVTOL model is that no limitation is imposed to its point of operation. This does not happen when the model is linearized at an operating point, because when working away from the operating point the system performance is not good. However, a PVTOL model also has a limitation: it is not possible to accomplish positioning tasks in the 3D space.

This work proposes an answer to this problem: a control structure that switches between different PVTOL controllers to achieve the goal of positioning a quadrotor, illustrated in Fig. 1(a), in the 3D space, where each controller is based on the Theory of Lyapunov. This work was developed considering that the system has a GPS. In this case, one specifies a sequence of points, and the helicopter should reach each one of such references. This idea is somewhat similar to path-following missions, an idea to be developed as future work. The contributions of the manuscript are: a) the proposition of a nonlinear controller suitable to accomplish positioning tasks in the 3D space based on three different PVTOL tasks; b) the proof of stability of the equilibrium of the closed-loop system considering such PVTOL tasks. To deal with such topics, Section II presents simplifications of the dynamic model of a mini-helicopter, after being extended for quadrotors, proposed in [11], in order to get a PVTOL model. Following, Section III discusses the controller proposed to stabilize the aircraft during flight, and Section IV presents experimental results obtained using the proposed controller to guide an ArDrone quadrotor. Finally, some concluding remarks are highlighted in Section V.

II. The Quadrotor Model

Commonly a rotorcraft machine can be split into four interconnected subsystems, which represent the actuator dynamics, the rotary-wing dynamics, the torque/forces generation and the rigid body dynamics [15], [16] (see Fig. 2). The first block associates joystick commands $\mathbf{u}$ to motor speeds ω, while the second one converts motor speed to thrust $\mathbf{f}$, taking into account the physical characteristics of the propellers. Following, in the third block the normal force produced by each motor is decomposed in forces and torques acting on the rigid body, resulting in a 3-D displacement (the fourth block).

Notice that the joystick commands entered to such system can be generated by RC controllers (human operator) or by a computer, through synthesized commands (autonomous navigation).

A. The Low- and High-Level Models

According to [17], which was validated in [18], the low-level dynamic model represented by the first two blocks in Fig. 2 can be approximated by a linear function, i.e., $\begin{bmatrix} u_\theta & u_\phi & u_\psi & u_z \end{bmatrix}^T = \alpha \begin{bmatrix} f_1 & f_2 & f_3 & f_4 \end{bmatrix}^T + \beta$, with $\alpha \in \mathbb{R}^4$ and $\beta \in \mathbb{R}^{4\times 1}$ being constant matrices. Another approach is to consider the white-box model that relates the joystick, motor, blade and thrust generation models, as described in [19], to servo commands sent to the motor thrusts.

The high-level dynamic model, representing the rigid body dynamics, can be obtained through Newton-Euler or Euler-Lagrange equations. In previous works [11] such model was detailed, in a way quite similar to the one in [20]–[22]. As one can check there, such model can be written as

$$\begin{bmatrix} m\mathbf{I} & \mathbf{0} \\ \mathbf{0} & \mathbf{M}_r(\eta) \end{bmatrix} \begin{bmatrix} \ddot{\xi} \\ \ddot{\eta} \end{bmatrix} + \begin{bmatrix} \mathbf{0} & \mathbf{0} \\ \mathbf{0} & \mathbf{C}_r(\eta,\dot{\eta}) \end{bmatrix} \begin{bmatrix} \dot{\xi} \\ \dot{\eta} \end{bmatrix} + \begin{bmatrix} \mathbf{G} \\ \mathbf{0} \end{bmatrix} = \begin{bmatrix} \mathbf{f} \\ \tau \end{bmatrix}, \tag{1}$$

where $\xi = \begin{bmatrix} x & y & z \end{bmatrix}^T \in \mathbb{R}^3$ indicates the longitudinal, lateral and normal displacements of the aircraft, and $\eta = \begin{bmatrix} \phi & \theta & \psi \end{bmatrix}^T \in \mathbb{R}^3$ indicates the angles of roll, pitch and yaw with respect to the inertial frame $\langle g \rangle$. By their turn, m is the total mass of the vehicle, $\mathbf{I} \in \mathbb{R}^{3\times 3}$ is a third-order identity matrix, $\mathbf{M}_r(\eta)$ represents the rotational matrix of inertia, $\mathbf{C}_r(\eta,\dot{\eta})$ is the rotational matrix of Coriolis and $\mathbf{G}$ is the vector of gravitational forces. The vectors of forces and torques applied to the aircraft are given by

$$\mathbf{f} = \begin{bmatrix} f_x \\ f_y \\ f_z \end{bmatrix} = \mathscr{R}\mathscr{A}_t \begin{bmatrix} f_1 \\ f_2 \\ f_3 \\ f_4 \end{bmatrix} \text{ and } \tau = \begin{bmatrix} \tau_\phi \\ \tau_\theta \\ \tau_\psi \end{bmatrix} = \mathscr{A}_r \begin{bmatrix} f_1 \\ f_2 \\ f_3 \\ f_4 \end{bmatrix},$$

respectively, where $\mathscr{R}$ is the 3D-rotation matrix relating the inertial frame $\langle g \rangle$ to the body frame $\langle b \rangle$, given by

$$\mathscr{R} = \begin{bmatrix} c_\psi c_\theta & c_\psi s_\theta s_\phi - s_\psi c_\phi & c_\psi s_\theta c_\phi + s_\psi s_\phi \\ s_\psi c_\theta & s_\psi s_\theta s_\phi + c_\psi c_\phi & s_\psi s_\theta c_\phi - c_\psi s_\phi \\ -s_\theta & c_\theta s_\phi & c_\theta c_\phi \end{bmatrix}, \tag{2}$$

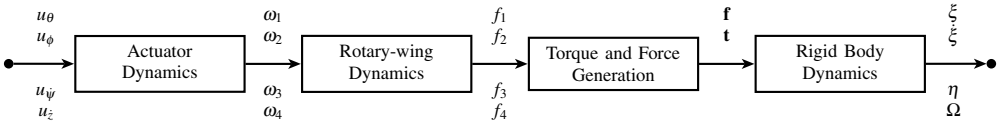

Fig. 2. Block diagram representing the dynamic model of a quadrotor.

where c_θ stands for $cos\theta$, s_θ stands for $sin\theta$, and so on.

The matrices $\mathscr{A}_t$ and $\mathscr{A}_r$ relate the thrusts applied at the body frame and the levers of the torque inputs, respectively, and are given by

$$\mathscr{A}_t = \begin{bmatrix} 0 & 0 & 0 & 0 \\ 0 & 0 & 0 & 0 \\ 1 & 1 & 1 & 1 \end{bmatrix} \text{ and } \mathscr{A}_r = \begin{bmatrix} k_1 & k_1 & -k_1 & -k_1 \\ -k_1 & k_1 & k_1 & -k_1 \\ k_2 & -k_2 & k_2 & -k_2 \end{bmatrix}.$$

Notice that all the four propellers point to the ${}^b z$ direction, as emphasized in $\mathscr{A}_t$. Moreover in $\mathscr{A}_r$, k_1 is the distance between the center of gravity (point of control) and the propeller, and k_2 represents the torque-thrust relationship.

In this work an ArDrone quadrotor is used. Differently of other prototypes found in the literature, their motors are not aligned with the ${}^b x$ and ${}^b y$ axes; in contrast, they are displaced 45 degrees with respect to the ${}^b z$ axis. As a consequence, it is necessary a coupled actuation of all motors to execute a lateral or longitudinal maneuver.

B. The High-Level PVTOL Model

PVTOL aircrafts are aerial vehicles having the capability to takeoff, hover and land vertically. In addition, those machines are able to execute flight missions in a vertical plane specified by a heading value. Such description was firstly introduced in [14], and even nowadays it continues being a benchmark for controller design in aerospace engineering, due to the control challenge for set-point stabilization and trajectory tracking guidance.

A quadrotor can be classified as a PVTOL aircraft. Thus, to accomplish a maneuver in the **XZ** plane, some constraints should be imposed. In such a case, one should guarantee that $\phi(t) = \psi(t) = 0 \ \forall t \geq 0$, as well as the correspondent angular velocities ($\dot{\phi} = \dot{\psi} = 0 \ \forall t \geq 0$). This means to guarantee that $f_y = 0$, $\tau_\phi = 0$ and $\tau_\psi = 0 \ \forall t \geq 0$. These actions restrict yaw and roll movements. On the other hand, to accomplish a maneuver in the **YZ** plane, it is necessary to guarantee that $\theta(t) = \psi(t) = 0 \ \forall t \geq 0$, with $\dot{\theta} = \dot{\psi} = 0 \ \forall t \geq 0$, since $f_x = 0$, $\tau_\theta = 0$ and $\tau_\psi = 0 \ \forall t \geq 0$. In such case, one guarantees restrictions on the pitch and yaw movements.

Moreover, if a VTOL (or a hovering) task should be accomplished in the **Z** axis, the x and y displacements should be physically restricted, i.e., longitudinal and lateral displacements are not allowed. In such case, $\phi(t) = \theta(t) = 0 \ \forall t \geq 0$, as well as the correspondent angular velocities are zero ($\dot{\phi} = \dot{\theta} = 0 \ \forall t \geq 0$). This means to guarantee that $f_x = 0$, $f_y = 0$, $\tau_\phi = 0$ and $\tau_\theta = 0 \ \forall t \geq 0$.

Considering PVTOL tasks in the **XZ** and **YZ** planes and in the **Z** axis, as illustrated in Fig. 1(b) and 1(c), the translational and rotational dynamic models of the aircraft is simplified to

$$\begin{bmatrix} m\ddot{x} \\ 0 \\ m(\ddot{z}+g) \end{bmatrix} = \begin{bmatrix} u\sin\theta \\ 0 \\ u\cos\theta \end{bmatrix} \qquad \begin{bmatrix} \tau_\phi \\ \tau_\theta \\ \tau_\psi \end{bmatrix} = \begin{bmatrix} 0 \\ I_{yy}\ddot{\theta} \\ 0 \end{bmatrix}, \quad (3)$$

$$\begin{bmatrix} 0 \\ m\ddot{y} \\ m(\ddot{z}+g) \end{bmatrix} = \begin{bmatrix} 0 \\ -u\sin\phi \\ u\cos\phi \end{bmatrix} \qquad \begin{bmatrix} \tau_\phi \\ \tau_\theta \\ \tau_\psi \end{bmatrix} = \begin{bmatrix} I_{xx}\ddot{\phi} \\ 0 \\ 0 \end{bmatrix}, \quad (4)$$

$$\begin{bmatrix} 0 \\ 0 \\ m(\ddot{z}+g) \end{bmatrix} = \begin{bmatrix} 0 \\ 0 \\ u \end{bmatrix} \qquad \begin{bmatrix} \tau_\phi \\ \tau_\theta \\ \tau_\psi \end{bmatrix} = \begin{bmatrix} 0 \\ 0 \\ I_{zz}\ddot{\psi} \end{bmatrix}, \quad (5)$$

respectively, where $u = \sum_{i=1}^{4} f_i$, $\tau_\theta = k_1(-f_1 + f_2 + f_3 - f_4)$, $\tau_\phi = k_1(f_1 + f_2 - f_3 - f_4)$, and $\tau_\psi = k_2(f_1 - f_2 + f_3 - f_4)$.

III. The PVTOL Controllers

This section presents three PVTOL controllers capable to guide a RUAV in the **XZ** and **YZ** planes and **Z** axis. These controllers can be understood as sub-controllers of a complete one, which is able to execute maneuvers without any flight constraint. Therefore, once proven the stability of the closed-loop system using a Lyapunov candidate function that incorporates all state pose variables ($\mathbf{q} = [\xi \ \ \eta]^T$), the controllers proposed for each sub-system (PVTOL systems) can be switched between them without loosing the stability, if the same Lyapunov candidate sub-functions are used to demonstrate their stabilities. This characterizes a switching controller considering a single unique Lyapunov function, as discussed in [23].

A. XZ-PVTOL Controller

In order to propose a positioning controller whose objective is to take the UAV from any initial position to a desired position, only using maneuvers in the **XZ** plane, it means to guarantee that $\begin{bmatrix} x & z & \theta & \dot{x} & \dot{z} & \dot{\theta} \end{bmatrix}^T \rightarrow \begin{bmatrix} x_d & z_d & \theta_d & \dot{x}_d & \dot{z}_d & \dot{\theta}_d \end{bmatrix}^T$, i.e., $\tilde{\mathbf{x}} \rightarrow \mathbf{0}$, where $\tilde{\mathbf{x}} = \mathbf{x} - \mathbf{x}_d$ is the current pose error.

In order to analyze the stability of the equilibrium $\tilde{\mathbf{x}} = \mathbf{0}$ correspondent to the closed-loop system, it is proposed the Lyapunov candidate function

$$V(\tilde{\mathbf{x}}) = \underbrace{K_{x2}\ln\cosh(K_{x1}K_{x2}^{-1}\tilde{x}) + \frac{1}{2}\dot{\tilde{x}}^2}_{V_1} + \underbrace{K_{z2}\ln\cosh(K_{z1}K_{z2}^{-1}\tilde{z}) + \frac{1}{2}\dot{\tilde{z}}^2}_{V2}$$
$$+ \underbrace{K_{\theta 2}\ln\cosh(K_{\theta 1}K_{\theta 2}^{-1}\tilde{\theta}) + \frac{1}{2}\dot{\tilde{\theta}}^2}_{V_3} > 0,$$

where K_{ij} are real positive gains.

The proposal here is to stabilize the altitude z and then to control its longitudinal displacement x through controlling its pitch angle θ. To do that it is necessary to write (3) in terms of the altitude control errors, i.e.,

$$\ddot{\tilde{z}} - \ddot{z}_d = g - \frac{u}{m}\cos\theta, \tag{6}$$

whose asymptotic stability is guaranteed by using the control signal

$$u = \frac{m}{\cos\theta}(\eta_z + g), \tag{7}$$

with $\eta_z = \ddot{z}_d + K_{z1}\tanh(K_{z1}K_{z2}^{-1}\tilde{z}) + K_{z3}\tanh(K_{z3}K_{z4}^{-1}\dot{\tilde{z}})$. Then, the closed-loop system description becomes

$$\ddot{\tilde{z}} + K_{z1}\tanh(K_{z1}K_{z2}^{-1}\tilde{z}) + K_{z3}\tanh(K_{z3}K_{z4}^{-1}\dot{\tilde{z}}) = 0. \tag{8}$$

To analyze the system stability using the theory of Lyapunov, one should obtain the first time derivative of $V_2(\tilde{z},\dot{\tilde{z}})$, and then replace (6) and (7) to get

$$\begin{aligned}\dot{V}_2(\tilde{z},\dot{\tilde{z}}) &= K_{z1}\tanh(K_{z1}K_{z2}^{-1}\tilde{z})\dot{\tilde{z}} + \dot{\tilde{z}}(\ddot{z}_d - \eta_z)\\ &= -K_{z3}\dot{\tilde{z}}\tanh(K_{z3}K_{z4}^{-1}\dot{\tilde{z}}) \leq 0.\end{aligned}$$

As one can see $\dot{V}_2(\tilde{z},\dot{\tilde{z}})$ is negative semi-definite. Then, $\tilde{z}$ and $\dot{\tilde{z}}$ are bounded, and it is possible to show that $\dot{\tilde{z}}$ is square integrable. In other words, $\tilde{z},\dot{\tilde{z}} \in L_\infty$ and $\dot{\tilde{z}} \in L_2$. Now, by applying the theorem of La Salle for autonomous systems, when observing the dynamics of the system characterized by (8), the greatest invariant set $\mathbf{M}$ in the region

$$\Omega = \left\{ \begin{bmatrix}\tilde{z}\\ \dot{\tilde{z}}\end{bmatrix} : \dot{V}_2(\tilde{z},\dot{\tilde{z}}) = 0 \right\} \Rightarrow \left\{ \begin{bmatrix}\tilde{z}\\ \dot{\tilde{z}}\end{bmatrix} = \begin{bmatrix}\tilde{z}\\ 0\end{bmatrix} \right\}$$

only takes place for $\tilde{z} = 0$. This way, the only invariant set $\mathbf{M}$ is the equilibrium $\begin{bmatrix}\tilde{z} & \dot{\tilde{z}}\end{bmatrix}^T = \begin{bmatrix}0 & 0\end{bmatrix}^T$, which is asymptotically stable. In other words, $\tilde{z}(t),\dot{\tilde{z}}(t) \to 0$ when $t \to \infty$.

Now, to stabilize the pitch angle it is proposed a tracking controller based on the theory of Lyapunov, whose objective is to track $\theta(t) \to \theta_d(t)$, with $\tilde{\theta} = \theta_d - \theta$. Taking the first temporal derivative of $V_3(\tilde{\theta},\dot{\tilde{\theta}})$,

$$\begin{aligned}\dot{V}_3(\tilde{\theta},\dot{\tilde{\theta}}) &= K_{\theta1}\tanh(K_{\theta1}K_{\theta2}^{-1}\tilde{\theta})\dot{\tilde{\theta}} + \dot{\tilde{\theta}}\ddot{\tilde{\theta}}\\ &= \dot{\tilde{\theta}}\left(K_{\theta1}\tanh(K_{\theta1}K_{\theta2}^{-1}\tilde{\theta}) + \ddot{\theta}_d - \frac{\tau_\theta}{I_{yy}}\right).\end{aligned}$$

Adopting and replacing the following control signal

$$\tau_\theta = I_{yy}\left(\ddot{\theta}_d + K_{\theta1}\tanh(K_{\theta1}K_{\theta2}^{-1}\tilde{\theta}) + K_{\theta3}\tanh(K_{\theta3}K_{\theta4}^{-1}\dot{\tilde{\theta}})\right),$$

one gets $\dot{V}_3(\tilde{\theta},\dot{\tilde{\theta}}) = -K_{\theta3}\dot{\tilde{\theta}}^2 \leq 0$, which is semi-definite negative. Thus, $\tilde{\theta},\dot{\tilde{\theta}} \in L_\infty$ and $\dot{\tilde{\theta}} \in L_2$. Taking (3) and analyzing the closed-loop system equation for the pitch angle

$$\ddot{\tilde{\theta}} + K_{\theta1}\tanh K_{\theta1}K_{\theta2}^{-1}\tilde{\theta} + K_{\theta3}\tanh K_{\theta3}K_{\theta4}^{-1}\dot{\tilde{\theta}} = 0,$$

after applying the theorem of La Salle for autonomous systems, one concludes that the greater invariant set $\mathbf{M}$ in

$$\Omega = \left\{ \begin{bmatrix}\tilde{\theta}\\ \dot{\tilde{\theta}}\end{bmatrix} : \dot{V}_3(\tilde{\theta},\dot{\tilde{\theta}}) = 0 \right\} \Rightarrow \left\{ \begin{bmatrix}\tilde{\theta}\\ \dot{\tilde{\theta}}\end{bmatrix} = \begin{bmatrix}\tilde{\theta}\\ 0\end{bmatrix} \right\}$$

exists uniquely for $\tilde{\theta} = 0$. Therefore, the equilibrium $\begin{bmatrix}\tilde{\theta} & \dot{\tilde{\theta}}\end{bmatrix}^T = \begin{bmatrix}0 & 0\end{bmatrix}^T$ of such system is asymptotically stable, i.e., $\tilde{\theta}(t),\dot{\tilde{\theta}}(t) \to 0$ when $t \to \infty$.

Finally, to complete the design of the **XZ**-PVTOL controller, it is necessary to guarantee the stability for the horizontal displacement, guiding it through θ_d. It is done representing (3) as

$$\ddot{\tilde{x}} = (\eta_z + g)\tan(\theta_d - \tilde{\theta}) - \ddot{x}_d, \tag{9}$$

after replacing (7). Considering a perfect pitch tracking ($\theta \equiv \theta_d | \tilde{\theta} \to 0$), adopting

$$\theta_d = \tan^{-1}\left[\frac{\ddot{x}_d + K_{x1}\tanh\left(K_{x1}K_{x2}^{-1}\tilde{x}\right) + K_{x3}\tanh\left(K_{x3}K_{x4}^{-1}\dot{\tilde{x}}\right)}{\eta_z + g}\right],$$

and then replacing it in (9), the closed-loop system equation becomes

$$\ddot{\tilde{x}} + K_{x1}\tanh(K_{x1}K_{x2}^{-1}\tilde{x}) + K_{x3}\tanh(K_{x3}K_{x4}^{-1}\dot{\tilde{x}}) = 0. \tag{10}$$

To analyze the stability of the equilibrium of such system based on the theory of Lyapunov, one takes the first time derivative of $V_1(\tilde{x},\dot{\tilde{x}})$, and then, using (10), it comes that

$$\begin{aligned}\dot{V}_1(\tilde{x},\dot{\tilde{x}}) &= K_{x1}\tanh(K_{x1}K_{x2}^{-1}\tilde{x})\dot{\tilde{x}} + \dot{\tilde{x}}\ddot{\tilde{x}}\\ &= -K_{x3}\dot{\tilde{x}}\tanh(K_{x3}K_{x4}^{-1}\dot{\tilde{x}}) \leq 0,\end{aligned} \tag{11}$$

thus getting the conclusion that $\tilde{x},\dot{\tilde{x}} \in L_\infty$ and $\dot{\tilde{x}} \in L_2$. As $\dot{V}_1$ is semi-definite negative, the theorem of La Salle allows to conclude that the closed-loop system described by (10) has, in the region

$$\Omega = \left\{ \begin{bmatrix}\tilde{x}\\ \dot{\tilde{x}}\end{bmatrix} : \dot{V}_1(\tilde{x},\dot{\tilde{x}}) = 0 \right\} \Rightarrow \left\{ \begin{bmatrix}\tilde{x}\\ \dot{\tilde{x}}\end{bmatrix} = \begin{bmatrix}\tilde{x}\\ 0\end{bmatrix} \right\},$$

the equilibrium $\begin{bmatrix}\tilde{x} & \dot{\tilde{x}}\end{bmatrix}^T = \begin{bmatrix}0 & 0\end{bmatrix}^T$ as its least invariant set $\mathbf{M}$. As a consequence, such equilibrium is asymptotically stable, so that $\tilde{x}(t),\dot{\tilde{x}}(t) \to 0$ when $t \to \infty$.

B. **YZ**-*PVTOL Controller*

To propose a positioning controller for flight tasks in the **YZ** plane, it should be guaranteed that $\begin{bmatrix}y & z & \phi & \dot{y} & \dot{z} & \dot{\phi}\end{bmatrix}^T \to \begin{bmatrix}y_d & z_d & \phi_d & \dot{y}_d & \dot{z}_d & \dot{\phi}_d\end{bmatrix}^T$, i.e., $\tilde{\mathbf{x}} \to \mathbf{0}$, where $\tilde{\mathbf{x}} = \mathbf{x} - \mathbf{x}_d$ is the current pose error. To analyze the stability of the equilibrium $\tilde{\mathbf{x}} = \mathbf{0}$, it is proposed the Lyapunov candidate function

$$\begin{aligned}V(\tilde{\mathbf{x}}) = \underbrace{K_{y2}\ln\cosh(K_{y1}K_{y2}^{-1}\tilde{y}) + \frac{1}{2}\dot{\tilde{y}}^2}_{V_1} + \underbrace{K_{z2}\ln\cosh(K_{z1}K_{z2}^{-1}\tilde{z}) + \frac{1}{2}\dot{\tilde{z}}^2}_{V_2}\\ + \underbrace{K_{\phi2}\ln\cosh(K_{\phi1}K_{\phi2}^{-1}\tilde{\phi}) + \frac{1}{2}\dot{\tilde{\phi}}^2}_{V_3} > 0,\end{aligned}$$

where K_{ij} are real positive gains.

In such case, the proposal is to stabilize the altitude z and then to control the lateral displacement y through controlling the roll angle ϕ. The analysis is quite similar to the one presented in Subsection III-A, thus it would be redundant to show the controller design and the stability proof once again.

Therefore, the control signals adopted to accomplish this new control objectives are directly presented, and are

$$u = \frac{m}{\cos\phi}(\eta_z + g),$$

with $\eta_z = \ddot{z}_d + K_{z1}\tanh(K_{z1}K_{z2}^{-1}\tilde{z}) + K_{z3}\tanh(K_{z3}K_{z4}^{-1}\dot{\tilde{z}})$,

$$\tau_\phi = I_{xx}\left(\ddot{\phi}_d + K_{\phi 1}\tanh(K_{\phi 1}K_{\phi 2}^{-1}\tilde{\phi}) + K_{\phi 3}\tanh(K_{\phi 3}K_{\phi 4}^{-1}\dot{\tilde{\phi}})\right),$$

$$\phi_d = \tan^{-1}\left[\frac{\ddot{y}_d + K_{y1}\tanh\left(K_{y1}K_{y2}^{-1}\tilde{y}\right) + K_{y3}\tanh\left(K_{y3}K_{y4}^{-1}\dot{\tilde{y}}\right)}{-(\eta_z + g)}\right],$$

which guarantee the asymptotical convergence of the state variables involved.

C. Z-PVTOL Controller

Considering now flight missions executed in the vertical axis, i.e., altitude and heading control, the RUAV model becomes a set of two independent linear systems, as (5) shows. In this sense, proposing the following control signals

$$u = m(\ddot{z}_d + K_{z1}\tanh(K_{z1}K_{z2}^{-1}\tilde{z}) + K_{z3}\tanh(K_{z3}K_{z4}^{-1}\dot{\tilde{z}}) + g),$$

$$\tau_\psi = I_{zz}\left(\ddot{\psi}_d + K_{\psi 1}\tanh(K_{\psi 1}K_{\psi 2}^{-1}\tilde{\psi}) + K_{\psi 3}\tanh(K_{\psi 3}K_{\psi 4}^{-1}\dot{\tilde{\psi}})\right),$$

we get the closed loop system

$$\ddot{\tilde{z}} + K_{z1}\tanh(K_{z1}K_{z2}^{-1}\tilde{z}) + K_{z3}\tanh(K_{z3}K_{z4}^{-1}\dot{\tilde{z}}) = 0,$$

$$\ddot{\tilde{\psi}} + K_{\psi 1}\tanh(K_{\psi 1}K_{\psi 2}^{-1}\tilde{\psi}) + K_{\psi 3}\tanh(K_{\psi 3}K_{\psi 4}^{-1}\dot{\tilde{\psi}}) = 0.$$

To analyze the stability, one can take the Lyapunov candidate function

$$V(\tilde{\mathbf{x}}) = K_{z2}\ln\cosh(K_{z1}K_{z2}^{-1}\tilde{z}) + \frac{1}{2}\dot{\tilde{z}}^2 + K_{\psi 2}\ln\cosh(K_{\psi 1}K_{\psi 2}^{-1}\tilde{\psi}) + \frac{1}{2}\dot{\tilde{\psi}}^2 > 0,$$

where K_{ij} are real positive gains, compute the first time derivative and replace the closed loop equation to get

$$\dot{V} = -K_{z3}\dot{\tilde{z}}\tanh(K_{z3}K_{z4}^{-1}\dot{\tilde{z}}) - K_{\psi 3}\dot{\tilde{\psi}}\tanh(K_{\psi 3}K_{\psi 4}^{-1}\dot{\tilde{\psi}}) \leq 0.$$

Observing that $\dot{V}$ is semi-defined negative, one can only conclude that $\tilde{z}, \tilde{\psi}, \dot{\tilde{z}}, \dot{\tilde{\psi}} \in L_\infty$, i.e., the state variables are bounded. In a way similar to that detailed in Subsection III-A, applying La Salle theorem for autonomous systems, the least invariant set $\mathbf{M}$ in the region Ω is the equilibrium, thus $\tilde{z}, \tilde{\psi}, \dot{\tilde{z}}, \dot{\tilde{\psi}} \in L_2$ and the state variables tend to zero for $t \to \infty$ asymptotically.

D. Switching Control Strategy

After designing PVTOL controllers to guide a quadrotor navigation in a vertical plane or normal axes in the global frame, it is necessary a switching strategy between them to perform a 3-D navigation. In other words, one should define a set of rules and then to propose a supervisor to manage them. The switching signal σ is split in the following stages:

- σ_1 To move forward to the desired position, executing forward maneuvers (**XZ**-PVTOL enabled);
- σ_2 To minimize lateral errors, executing lateral corrective maneuvers (**YZ**-PVTOL enabled);
- σ_3 To reduce the heading error (**Z**-PVTOL enabled).

The supervisor is responsible for analyzing some cases and for deciding the suitable switching signal.

- C_1 If the heading error is lower than $\tilde{\psi}_{\min}$ and the lateral error is lower than $\tilde{y}_{\min}$, then σ_1 is activated;
- C_2 If the heading error is lower than $\tilde{\psi}_{\min}$ and the lateral error is greater than $\tilde{y}_{\min}$, then σ_2 is activated.
- C_3 If the desired position (x_d, y_d, z_d) changes or the heading error is greater than $\tilde{\psi}_{\min}$, then the current yaw value should be corrected and σ_3 is activated;

In a certain way, such simpler controllers could be considered as part of a complete one. The result is that using such strategy the aircraft can follow piecewise linear paths, stopping moving ahead for correcting any lateral displacement and orientation. The advantage of such proposal is that the entire controller thus obtained is much simpler to implement then a 3D nonlinear controller. A disadvantage is that because of the stops to correct the aircraft heading and the lateral displacements the mission accomplishment takes more time.

IV. Experimental Results and Discussion

This subsection presents a set-point stabilization experiment for a quadrotor in the 3D space, using the controller designed in Section III. The closed-loop stability is also demonstrated during a flight mission considering the switching conditions detailed in Subsection III-D. The quadrotor used is an ArDrone Parrot, whose parameters are shown in Table I (in [24] one can found the set of sensors onboard this RUAV and its utility in the robotic research field). Complementing the experimental setup, a Software Development Kit (SDK) available at the ArDrone Parrot web site, links the Matlab© code running in an external computer and the RUAV.

Figures 3 and 4 illustrate the time evolution of the rotorcraft posture during the 3-D positioning mission, as well as the abstract and the real control signals (respectively the desired forces, defined by the high-level controller, and the inputs accepted by the vehicle, defined by the low-level controller) applied to guide it. The real/abstract input relationship used in this work follows quite closely the development presented in [19]. Such step is here labeled as low-level dynamic model, as explained in Section II.

TABLE I
ARDRONE PARAMETERS

$m = 0.380[kg]$	$k_1 = 0.1782[m]$	$k_2 = 0.0290[m]$
$I_{xx} = 0.0957[kgm^2]$	$I_{yy} = 0.01857[kgm^2]$	$I_{zz} = 0.0255[kgm^2]$

In order to compare the performance of the proposed controller, an underactuated nonlinear controller based on partial feedback linearization [11] is also implemented and run, considering the whole dynamics of the RUAV (all the six degrees of freedom are simultaneously controlled).

The experiment run consists in a set-point stabilization, which changes in the desired 3-D position occurring every $25s$, with the RUAV reaching the waypoints $x_d = [0,\ 2,\ 0,\ -2,\ -2,\ 0]$, $y_d = [0,\ 2,\ 4,\ 2,\ -2,\ -4]$, and $z_d = [1,\ 2,\ 1,\ 2,\ 1,\ 2]$. The yaw reference is calculated whenever some desired position changes, and is given by $\psi_d = \tan^{-1}\left(\frac{y_d[k]-y_d[k-1]}{x_d[k]-x_d[k-1]}\right)$.

As for the graphics in Figures 3 and 4, the red lines correspond to the results got with the switching PVTOL controller here proposed, whereas the blue lines correspond to the results got the underactuated controller proposed in [11]. The dashed-lines indicate the desired values, which are the same for both controllers.

Despite having different delays between the controllers to accomplish longitudinal/lateral displacement, both reach the reference asymptotically, as expected. In addition, it is possible to check in Fig. 3 that the results for altitude and yaw control are practically identical, what can be justified by the fact that such variables are not strongly coupled to the other variables. One can also notice in Fig. 4(a) that at intervals of $25s$ all forces increase/decrease jointly, due to the altitude reference change (see Fig. 3(a)), an effect that can also be observed in Fig. 4(b), in the $\dot{z}$ real input.

Finally, it is also possible to verify that the underactuated nonlinear controller is not perfectly tuned. One can observe some bounded oscillations when the reference is reached (steady state). In this sense, an additional advantage of the switching PVTOL controller here proposed is its tuning easiness, once it is structurally much simpler. In fact, its simplicity allows implementing it onboard an aircraft with low-entry computational setup, a meaningful advantage in comparison with other controllers, like the one proposed in [11], for instance.

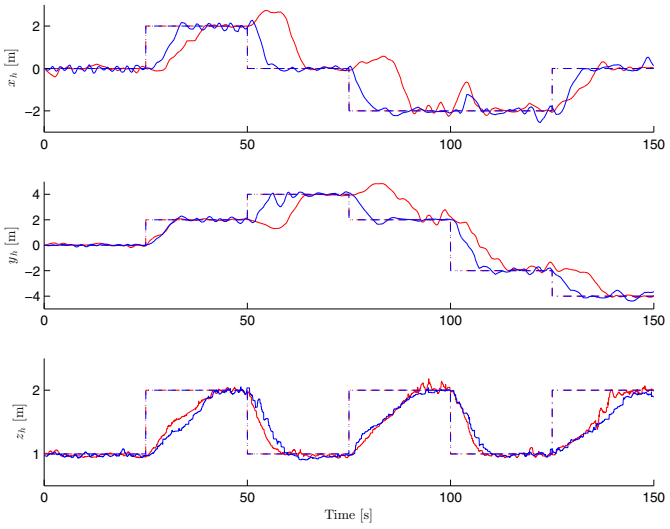

(a) RUAV position.

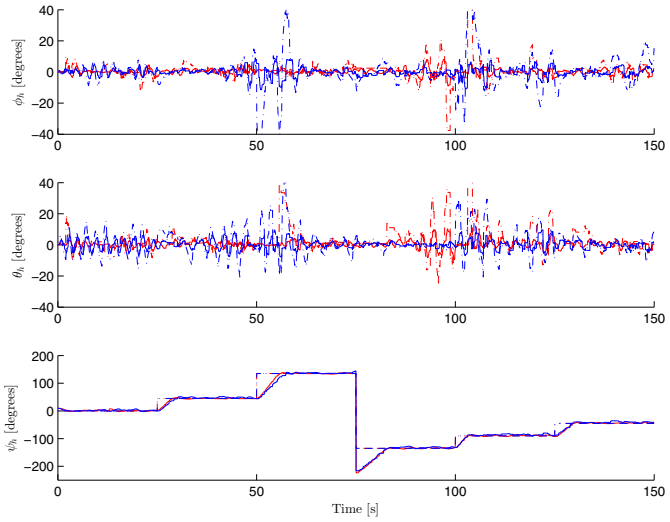

(b) RUAV orientation.

Fig. 3. Experimental result: Time evolution of the posture variables.

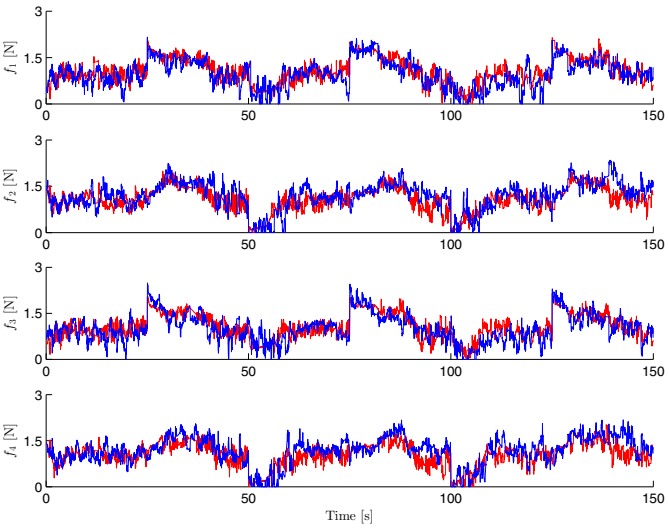

(a) Abstract control inputs.

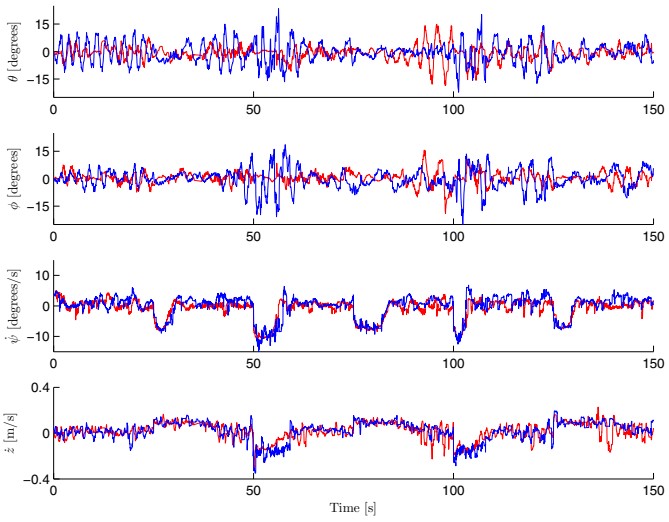

(b) Real control inputs.

Fig. 4. Experimental result: Time evolution of the control inputs.

To conclude the discussion on the results presented here, one should observe that the PVTOL-based switching controller here proposed responds more slowly than the complete controller, what is caused by the way it operates. First it accomplishes a task correspondent to re-orientation, if necessary, after every lateral movement, before starting the longitudinal movement. In contrast, for the complete controller all these steps are combined. However, in the strategy here proposed there is no aggressive maneuver. Moreover, an intrinsic limitation is that the controller here proposed can not accomplish trajectory-tracking missions, due to the temporary yaw restriction, which makes impossible to the switching PVTOL-based controller to follow the trajectory. Nevertheless, such controller is capable of accomplishing path-following missions, thus being suitable to work in outdoor environments, using global sensors. Thus, the next step of this research is to implement a controller to accomplish path-following missions using the strategy here proposed. To do that, the path to be followed will be approximated by for linear interpolations, generating a piecewise-linear version of the real path.

V. Concluding Remarks

In this work a switching strategy based on PVTOL controllers is proposed to guide a rotorcraft during 3-D navigation. The proposal is to orientate the rotorcraft to the desired point (using the **Z**-PVTOL controller) and then to guide it to reach such point (using the **XZ**-PVTOL controller) through longitudinal maneuvers, considering the body reference frame. If during such approach a lateral displacement error greater than a threshold value is observed, then the **YZ**-PVTOL controller is adopted to minimize it. The stability proof of each of such sub-systems is also included, as well as a strategy to switch between them without affecting the stability of the whole system. Experimental results validate the proposal, stressing that a set of simpler controllers is capable of guiding a RUAV in a more complex mission.

ACKNOWLEDGMENT

The authors thank CNPq for the financial support granted to this work (grant 474.467/2010-4). They also thank CAPES and SPU, which have supported the stay of Mr. Brandão in San Juan, Argentina, and Mr. Rosales in Vitória-ES, Brazil. Mr. Brandão also thanks Federal University of Viçosa, Brazil, and FAPEMIG for supporting his participation in this work. Mr. Rosales also thanks CONICET/Argentina for his doctoral scholarship.

References

[1] H. Eisenbeiss, "A mini unmanned aerial vehicle (uav): System overview and image acquisition," in *Proceedings of the International Workshop on Processing and Visualization Using High-Resolution Imagery*, Pitsanulok, Thailand, 2004.

[2] Y. Bestaoui and R. Slim, "Maneuvers for a quad- rotor autonomous helicopter," in *AIAA Conference and Exhibit*, Rohnert Park, California, May 7-10 2007.

[3] S. Rathinam, A. Kim, Z. Soghikian, and R. Sengupta, "Vision based following of locally linear structures using an unmanned aerial vehicle," in *Proceedings of the 44th IEEE Conference on Decision and Control, 2005 European Control Conference*, December 2005, pp. 6085–6090.

[4] E. MacArthur, D. MacArthur, and C. Crane, "Use of cooperative unmanned air and ground vehicles for detection and disposal of mines," in *Proceedings of the VI Intelligent Systems in Design and Manufacturing*, vol. 5999, 2005, pp. 94–101.

[5] F. Kendoul, "Survey of advances in guidance, navigation, and control of unmanned rotorcraft systems," *Journal of Field Robotics*, vol. 29, no. 2, pp. 315–378, 2012.

[6] L. Marconi and R. Naldi, "Robust nonlinear control of a miniature helicopter for aerobatic maneuvers," in *Proceedings of the 32nd Rotorcraft Forum*, 2006.

[7] F. Kendoul, "Optic flow-based vision system for autonomous 3d localization and control of small aerial vehicles," *Robotics and Autonomous Systems*, vol. 57, 2009.

[8] T. Madani and A. Benallegue, "Control of a quadrotor mini-helicopter via full state backstepping technique," in *Proc. 45th IEEE Conference on Decision and Control*, 2006.

[9] D. Mellinger and V. Kumar, "Minimum snap trajectory generation and control for quadrotors," in *Proccedings of the IEEE International Conference on Robotics and Automation*, May 2011.

[10] P. Castillo, A. Dzul, and R. Lozano, "Real-time stabilization and tracking of a four-rotor mini rotorcraft," in *Proceeding of the IEEE Transactions on Control Systems Technology*, vol. 12, no. 4, July 2004, pp. 510–516.

[11] A. S. Brandão, M. Sarcinelli-Filho, and R. Carelli, "A nonlinear underactuated controller for 3d-trajectory tracking with a miniature helicopter," in *IEEE International Conference on Industrial Technology (ICIT)*, 2010, pp. 1421–1426.

[12] A. S. Brandao, J. A. Sarapura, E. M. de O. Caldeira, M. Sarcinelli-Filho, and R. Carelli, "Decentralized control of a formation involving a miniature helicopter and a team of ground robots based on artificial vision," in *Proceedings of the 2010 Latin American Robotics Symposium and Intelligent Robotics Meeting*, 2010, pp. 126–131.

[13] P. Castillo, R. Lozano, and A. Dzul, "Experimental implementation of linear and nolinear control laws," *IEEE Control System Magazine*, pp. 45–55, December 2005.

[14] J. Hauser, S. Sastry, and G. Meyer, "Nonlinear control design for slightly non-minimum phase systems: Application to v/stol aircraft," *Automatica*, vol. 28, pp. 665–679, 1992.

[15] T. John and S. Sastry, "Differential flatness based full authority helicopter control design," in *Proceedings of the 38th Conference on Decision & Control*, Phoenix, Arizona, USA, December 1999, pp. 1982–1987.

[16] B. Ahmed, H. R. Pota, and M. Garratt, "Flight control of a rotary wing uav using backstepping," *International Journal of Robust and Nonlinear Control*, vol. 20, pp. 639–658, January 2010.

[17] M. Bernard, K. Kondak, N. Meyer, Y. Zhang, and G. Hommel, "Elaborated modeling and control for an autonomous quad-rotor," in *Proceedings of the 22nd International Unmanned Air Vehicle Systems Conference*, Bristol, UK, April 16-18 2007, pp. 2375–2380.

[18] L. V. Santana, A. S. Brandão, M. Sarcinelli-Filho, and R. Carelli, "Hovering control of a miniature helicopter attached to a platform," in *Proceedings of the 20th IEEE International Symposium on Industrial Electronics*, Gdansk, Poland, June 27-30 2011, pp. 2231–2236.

[19] A. S. Sanca, P. J. Alsina, and J. de Jesus F. Cerqueira, "Dynamic modeling of a quadrotor aerial vehicle with nonlinear inputs," in *Proceedings of the 5th Latin American Robotic Symposium*. Salvador, Brazil: IEEE Computer Society, 2008, pp. 143–148.

[20] S. K. Kim and D. M. Tilbury, "Mathematical modeling and experimental identification of a model helicopter," in *Proceedings of the AIAA Modeling and Simulation Technologies Conference and Exhibit*, Boston, MA, USA, 1998, pp. 203–213.

[21] P. Castillo, R. Lozano, and A. Dzul, *Modelling and Control of Mini-Flying Machines*. USA: Springer, 2005.

[22] G. V. Raffo, M. G. Ortega, and F. R. Rubio, "An integral predictive/nonlinear $\mathscr{H}_\infty$ control structure for a quadrotor helicopter," *Automatica*, vol. 46, pp. 29–39, 2010.

[23] J. M. Toibero, F. Roberti, R. Carelli, and P. Fiorini, "Switching control approach for stable navigation of mobile robots in unknown environments," *Robotics and Computer-Integrated Manufacturing*, vol. 27, no. 3, pp. 558 – 568, 2011.

[24] T. Krajník, V. Vonásek, D. Fišer, and J. Faigl, "AR-Drone as a Platform for Robotic Research and Education," in *Research and Education in Robotics: EUROBOT 2011*. Heidelberg: Springer, 2011.